



# Addressing Short Trapped-Flux Lifetime in High-Density Field-Reversed Configuration Plasmas in FRCHX\*

Chris Grabowski, James H. Degnan, David J. Amdahl, Matthew Domonkos, Edward L. Ruden, William White, Glen A. Wurden, Michael H. Frese, Sherry D. Frese, J. Frank Camacho, Sean K. Coffey, Gerald F. Kiuttu, Mark Kostora, John McCullough, Wayne Sommars, Alan G. Lynn, Kevin Yates, Bruno S. Bauer, Stephan Fuelling, Richard E. Siemon

**Abstract**—The objective of the Field-Reversed Configuration Heating Experiment (FRCHX) is to obtain a better understanding of the fundamental scientific issues associated with high energy density laboratory plasmas (HEDLPs) in strong, closed-field-line magnetic fields. These issues have relevance to such topics as magneto-inertial fusion (MIF), laboratory astrophysical research, and intense radiation sources, among others. To create HEDLP conditions, a field-reversed configuration (FRC) plasma of moderate density is first formed via reversed-field theta pinch. It is then translated into a cylindrical aluminum flux conserver (solid liner), where it is trapped between two magnetic mirrors and then compressed by the magnetically-driven implosion of the solid liner. A requirement is that once the FRC is stopped within the solid liner, the trapped flux inside the FRC must persist while the compression process is completed. With the present liner dimensions and implosion drive bank parameters, the total time required for implosion is  $\sim 25 \mu\text{s}$ . Lifetime measurements of recent FRCHX FRCs indicate trapped lifetimes now approaching  $\sim 14 \mu\text{s}$ . By separating the Mirror and Translation coil banks into two so that the mirror fields can be set lower initially, the liner compression can now be initiated 7-9  $\mu\text{s}$  before FRC formation begins. A discussion of FRC lifetime-limiting mechanisms and various experimental approaches to extending the FRC lifetime will be presented.

**Index Terms**—plasmas, plasma generation, plasma properties, inertial confinement, magnetic confinement

\* This work is supported by U.S. Department of Energy's Office of Fusion Energy Science

C. Grabowski (email: [chrisgrabowski@mailaps.org](mailto:chrisgrabowski@mailaps.org)), J. H. Degnan, D. J. Amdahl, M. Domonkos, E. L. Ruden, and W. White are with the Air Force Research Laboratory, Directed Energy Directorate, 3550 Aberdeen Ave SE, Kirtland AFB, NM 87117 USA.

G. A. Wurden is with Los Alamos National Laboratory, Magnetized Plasma Team, P-24, Los Alamos, NM 87545 USA.

M. H. Frese, S. D. Frese, J. F. Camacho, and S. K. Coffey are with NumerEx, LLC, 2309 Renard Place SE, Suite 220, Albuquerque, NM 87106 USA.

G. F. Kiuttu is with VariTech Services, 2901 Juan Tabo Blvd NE, Suite 121-B, Albuquerque, NM 87112 USA.

M. Kostora, J. McCullough, and W. Sommars are with Science Applications International Corporation, 2109 Air Park Road SE, Albuquerque, NM 87106 USA.

A. G. Lynn is with the University of New Mexico, Department of Electrical and Computer Engineering, Albuquerque, NM 87131 USA.

K. Yates, B.S. Bauer, S. Fuelling, and R.E. Siemon are with the University of Nevada, Reno, Physics Department, Reno, NV 89557 USA.

## I. INTRODUCTION

MAGNETO-INERTIAL FUSION (MIF) is an approach to Inertial Confinement Fusion (ICF) that takes advantage of embedded magnetic fields in the target plasma to reduce thermal conduction losses relative to conventional ICF techniques, thereby improving the plasma energy confinement. As a consequence, the required precision, speed, and density-radius product of the implosion for MIF is reduced, as well as the final convergence ratio [1]. Since 2008, the Air Force Research Laboratory (AFRL) and Los Alamos National Laboratory (LANL) have been working on the development of one version of MIF that uses a Field-Reversed Configuration (FRC) plasma, formed by a reversed-field theta pinch, for a target. The FRC is compressed via an imploding metal flux conserver or solid liner that is driven by an axial current (Z-pinch) discharge through the liner [1-4]. Experiments have demonstrated (1) reliable formation, translation, and capture of FRC plasmas within magnetic mirrors located inside the solid liners [5]; (2) implosion of liners with such magnetic mirror fields inside them, which provided evidence of compression of 1.36 T fields to fields up to 540 T [5]; (3) performance of a full system experiment of FRC formation, translation, capture, and solid liner compression [5]; and (4) identification (by comparison with 2D-MHD MACH2 simulations) of various factors limiting the closed-field lifetime of FRCs to about half that required for good liner compression to high energy density plasma (HEDP) conditions [6-8].

The latter has led to the design and preparation of various systems on the experiment intended to increase the FRC closed-field lifetime to an amount necessary to allow the plasma to undergo the full compression provided by the solid liner. Experiments with these new systems are now underway and have had the goal of at least doubling the FRC closed-field lifetimes in the capture region. These lifetimes, as reported at the 2011 IEEE International Pulsed Power Conference, were initially 7~9  $\mu\text{s}$  [6], and as will be discussed shortly this goal has largely been met with recent data showing captured FRC lifetimes now approaching 14~16  $\mu\text{s}$ .

Also during the course of performing experiments, imaging evidence of FRC instabilities was obtained; the use of stability control measures appears to have slowed and possibly stopped such instabilities.

The next section of this paper provides background information on FRC plasmas and describes the Field-Reversed Configuration Heating Experiment (FRCHX). Section III then discusses several potential issues that have been identified through comparison of experimental data and modeling as possibly contributing to short FRC trapped-flux lifetimes. Various techniques and systems that have been implemented to lengthen the FRC lifetime are discussed in Section IV, along with recent experimental data showing the improvements that have been obtained. Recent computational modeling results are shown next in Section V, which identify practices that can be employed to somewhat lessen the strict FRC lifetime requirements initially established. Finally, in Section VI a summary of the recent results is provided along with some concluding remarks.

## II. THE FRC PLASMA AND FRCHX

FRC plasmas are prolate compact toroidal plasmas that were investigated as early as the 1960's (see, e.g., [9]), yet they continue to be of considerable interest to the present day for fusion energy concepts because of their many positive attributes [10]. With FRCHX, and its sister experiment FRX-L at LANL [2], FRC plasmas are formed via a reversed-field theta pinch process. Figure 1 illustrates the basic steps to the formation.

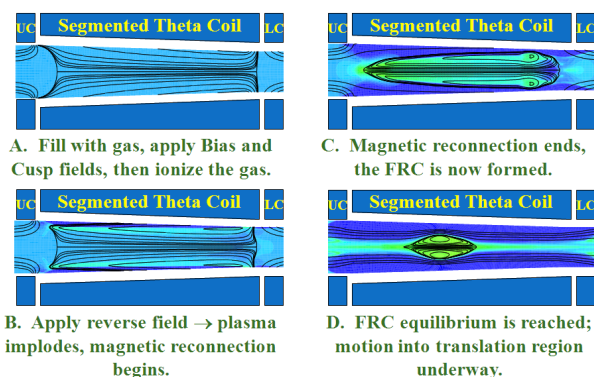


Figure 1. Description of FRC formation within the conical “segmented theta coil” of FRCHX. The black lines show surfaces of constant magnetic flux density.

A low-pressure background of  $D_2$  gas is first puffed into the quartz tube vacuum vessel from below the formation region to establish a mean fill of 35 ~ 75 mTorr within the bore of the theta pinch field coil (Figure 1a). Next, a quasi-DC Bias field is set up within the coil, followed shortly by cusp fields at either end. The  $D_2$  gas is then ionized by superimposing a high-frequency (~250 kHz) ringing Pre-Ionization (PI) field onto the Bias field using the same theta pinch coil. Once the gas is ionized, the Main field, which is oriented opposite to the Bias field, is applied to the theta coil to compress the plasma that was just formed (Figure 1b). Because of the earlier

application of the cusp fields, the Bias field abruptly exits the vacuum vessel at either end of the theta coil. According to simulations, the steering of the Bias field out of the vessel close to the coil provides for an efficient means of promoting the magnetic tearing and reconnection of Bias and Main field lines necessary to form the FRC, as the process is able to take place outside the quartz tube in a region absent of any conductive plasma. Once the Bias field lines in the plasma have reconnected to the interior Main field lines, the newly formed FRC continues to contract, as the Main field continues to increase (Figure 1c). Eventually, an equilibrium is reached between the external magnetic field pressure and the plasma and magnetic pressure interior to the FRC, and the compression stops (Figure 1d). Because the bore of the theta pinch field coil is conical, however, a net axial force is applied while the compression is occurring, and so by the time the radial equilibrium is reached, the FRC has gained considerable momentum and is exiting the formation region.

Once the FRC leaves the formation region, it enters a short translation region where the Translation fields (set up prior to formation) keep the FRC at approximately the same radial equilibrium as at the exit end of the formation region (Figure 2). The translation region leads to a capture region that is co-located with the solid liner used to compress the FRC. Magnetic mirrors at either end of the liner, also set up before formation, enable the FRC to be captured within the liner.

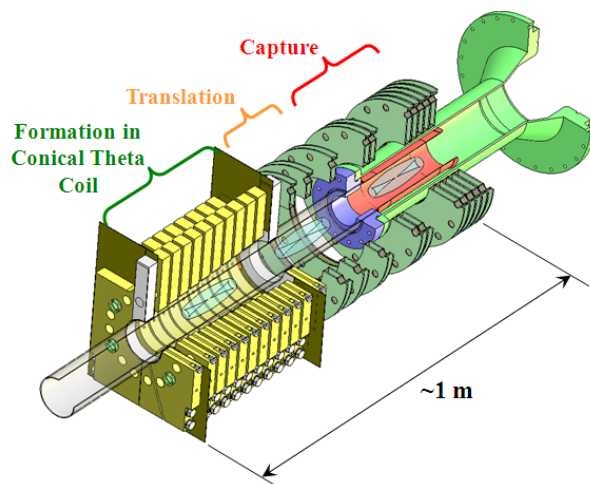


Figure 2. Illustration of the general layout of FRCHX.

Capture of the FRC is possible, as the first magnetic mirror has an amplitude slightly less than the mean field produced by the Main bank within the theta coil. The kinetic energy imparted to the FRC from the Main bank is then sufficient for the FRC to pass through the lower mirror and enter the well, but it is insufficient to allow it to slip past the upper mirror. Furthermore, because the reflection from the upper mirror is inelastic, some of the FRC's kinetic energy is lost through conversion to thermal energy after “hitting” the mirror. The result is that the FRC is unable to travel past the lower mirror again to leave the capture region. A slight increase in its temperature is also expected from this conversion.

Once captured the FRC is either diagnosed until it decays,

or it is compressed and heated by imploding the solid liner around it. The solid liner is an aluminum cylinder 30 cm in length and with an inner diameter of 9.78 cm. Because apertures are needed at both the bottom (for FRC entry into the capture region) and the top (for diagnostic access), the current contacts on either end of the liner are deformable. As such, the wall thickness of the liner is tapered near the ends, transitioning from a uniform 1.1 mm along the middle 18 cm of the liner, to 5 mm within 1cm of each end, and then finally to a 1-cm wall thickness at each end [4].

Compression of the FRC is accomplished as the magnetic fields produced by the induced image currents in the liner interior press inward on the FRC as the liner implodes. Because the aluminum liner is a flux excluder, almost all of the interior magnetic flux, including the magnetic mirror and well structure, is compressed along with the plasma. Figure 3 shows a MACH2 calculation of liner inner and outer wall radii, the peak magnetic flux density (at the upper mirror peak), and the implosion drive current provided by Shiva Star [4]. Also indicated on the graph are the liner inner and outer radii measured from radiographs taken during a liner implosion test performed on magnetic field only. Very good agreement is observed between the measured and calculated radii.

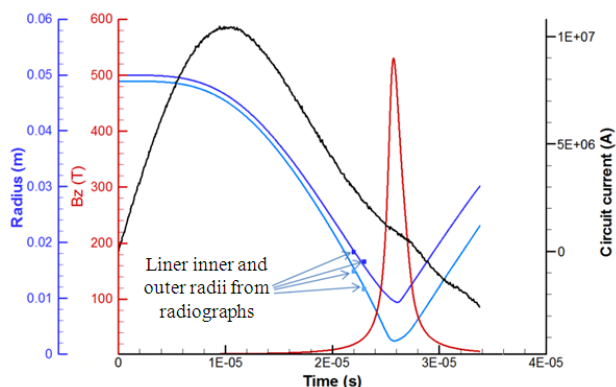


Figure 3. MACH2 calculation of solid liner implosion on vacuum magnetic field. Measured liner radii from such an implosion test are shown for comparison [5,8].

For an initial peak upper mirror field of 1.36 T, the calculation shows that the field increases by almost a factor of 400 to 540T, and the inner radius decreases to  $\sim 2.5$  mm, indicating a factor of  $\sim 19$  in compression. For the first 4  $\mu$ s of the implosion, however, there is negligible change in the liner radius, and at 10  $\mu$ s the radius has decreased only  $\sim 3.5$  mm or  $\sim 7\%$ . With this relatively slow start to the implosion, the time required to reach the minimum radius with this drive current is 25–26  $\mu$ s. The trapped flux must persist within the FRC at this time if the FRC is to be kept confined and allowed to undergo maximum compression. The first FRCHX implosion experiment performed in April 2010 failed to show signatures of compression, and it is believed that this was due to insufficient FRC lifetime. The next section presents several factors that can limit FRC lifetime.

### III. LIFETIME LIMITING FACTORS FOR TRAPPED FLUX WITHIN THE FRC

Through extensive comparison of computational and analytical results with experimental data, it became apparent that a number of potential situations existed that could affect FRC lifetime throughout the experimental system, from the formation region (where poor or delayed ionization could reduce the amount of Bias flux initially trapped within the FRC), through the translation region (where instabilities might develop), and into the capture region (where not only instabilities may affect the FRC but the profile of the mirror fields and incoming impurities, as well). These are not all of the factors that can influence the trapped-flux lifetime, however they appear to be the most likely ones influencing the FRC lifetimes in FRCHX. These lifetime-limiting issues are examined in further detail in the following sub-sections.

#### A. Poor Formation/Inadequate Flux Trapping

According to the FRC formation concept illustrated in Figure 1, the  $D_2$  gas is broken down uniformly throughout the formation region as soon as the ringing PI field is applied. The actual breakdown processes are different from this “ideal” process, however. First, the initial gas breakdown does not occur simultaneously or uniformly at every location throughout the formation region. Instead, the plasma first forms in a hollow annulus near the wall of the quartz tube and close to the middle of the theta coil. Secondly, the breakdown of the gas does not occur when the PI electric field is highest nor when there is a substantial background Bias field present but rather when the PI magnetic field has nearly negated the Bias field.

The photograph in Figure 4 shows an axial view of the FRCHX vacuum vessel and clearly illustrates the annular nature of the initial gas breakdown. The image has a 250-ns exposure, starting approximately 15 ns before the PI discharge begins on a test in which only the ringing PI field was applied to a 50-mTorr uniform  $D_2$  fill in the quartz tube. With the exception of some plasma that has drifted radially inward into the volume near the bottom of the photo, the gas breakdown is confined exclusively to the inside surface of the quartz vacuum vessel.

The B-dot and optical fiber probe data plotted in Figure 5 illustrate the timing of the breakdown relative to the applied fields. Shown in the graph are the waveforms from one of the formation region B-dot probes (“F”, which is located very near the middle of the formation region) and one of the optical fiber probes located at the same axial position. The time base is such that the Bias bank is triggered at  $t \sim -130$   $\mu$ s, and the PI bank is triggered at  $t \sim 0$   $\mu$ s. As is indicated by the arrow, the first visible-light emissions, or “first light”, detected by the optical fiber probe occur only when the net magnetic field has dropped to  $\sim 0.1$  T, or  $\sim 25\%$  of the initial Bias field. The delay in breakdown appears to be due to magnetic insulation effects; that is, the Bias field needed for FRC formation is actually inhibiting the initial breakdown. The result is that a much smaller percentage of the Bias field than what is available is actually getting embedded within the plasma. With less

trapped flux, the FRC's trapped flux lifetime will be shorter for any given resistive decay rate for the flux in the plasma.

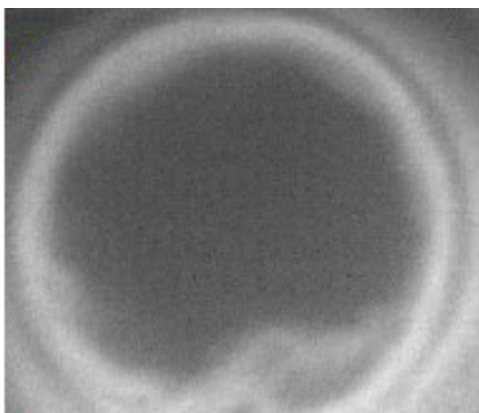


Figure 4. Photograph (250 ns exposure) showing an axial view of the annular breakdown in the  $D_2$  gas just after the PI bank discharge.

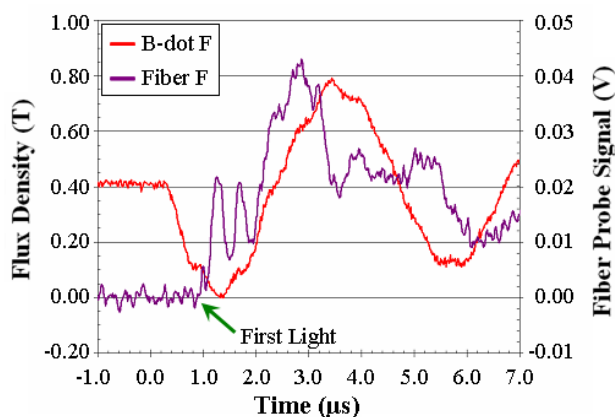


Figure 5. Overlay of B-dot and optical fiber waveforms showing initial plasma breakdown occurring when the net axial B field is just  $\sim 25\%$  of the applied Bias field.

### B. Late-Time Instabilities

Instabilities most likely to affect FRCs are the tearing ( $n=0$ ), tilt/wobble (" $n=1$ "), and rotational (" $n=2$ ") instabilities [10]. Multi-chord interferometry can give evidence, though not conclusive proof, of the first two simply through comparison of off-axis density with on-axis density. Figure 6 shows line-integrated density measurements made along three chords in the middle of the capture region (as well as a diameter chord measurement made in the middle of the formation region). The time  $t = 0 \mu s$  again corresponds to the time when the PI bank discharge begins; the Main bank discharge begins approximately  $3.1 \mu s$  later. For this shot, the diameter chord in the capture region (red) shows an abrupt slope change at  $15 \mu s$  and then drops abruptly at  $17 \mu s$ , while the off-diameter-chord measurements remain flat or increase slightly. These behaviors are suggestive of the FRC moving off-axis, perhaps due to tilt or wobble.

Figure 7 shows visible-light fast framing camera images from an earlier test that illustrate similar behavior. Each frame has a 100-ns exposure, and there is  $1 \mu s$  between the start of each frame. As indicated in the frame 1 image, the frame 1

exposure starts  $10 \mu s$  after the start of the PI bank discharge. This time roughly corresponds to when the front of the FRC reaches the middle of the capture region. The B-dot probe signal in the middle of the capture region then peaks at  $\sim 16 \mu s$ , corresponding approximately to the time at which frame 7 is taken. Viewing the images in sequence, they show a period of straight translation for the FRC (frames 1-6), followed by the onset of a transverse motion to the left (frames 7 – 10), and the finally what appears to be an impact on the wall (frames 11 – 12). The object lighting up near the FRC impact area in frames 10 – 12 is one of the B-dot probes inserted near the peak of the lower mirror field.

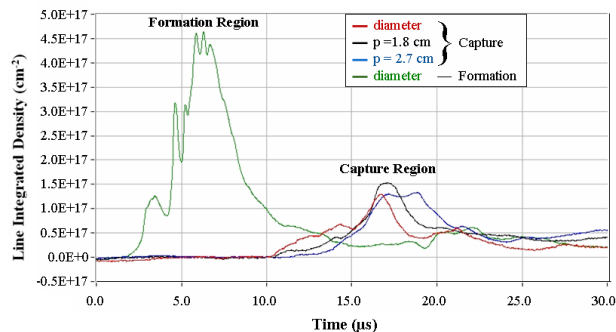


Figure 6. Multi-chord interferometry measurements showing the possible onset of an instability after capture.

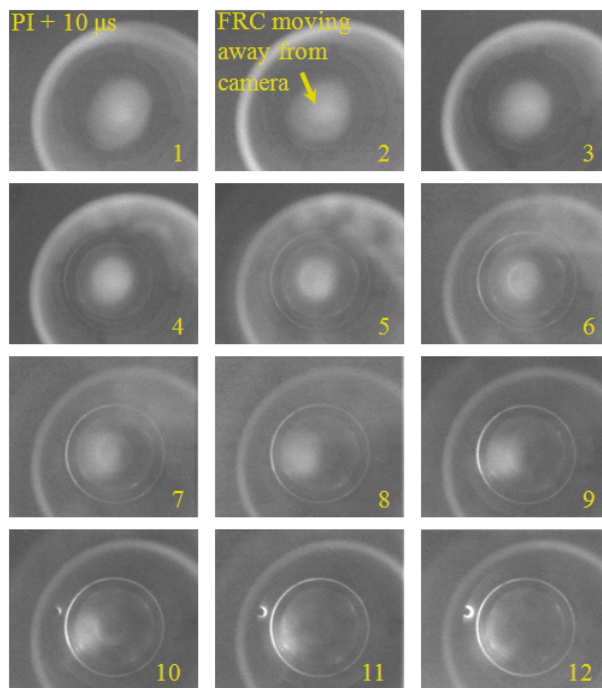


Figure 7. Fast-framing camera images showing late-time off-axis loss of the FRC. A probe is seen glowing in frames 10-12).

### C. Capture Region Field Profile Not Adequate

Magnetic probe signals along the translation and capture regions indicate that the FRC does appear to be successfully translated and captured but there may be mass and flux loss occurring during the capture, perhaps because the magnetic

profile may not be totally appropriate to hold the FRC at an equilibrium state. To illustrate these concerns, Figure 8 shows the magnetic probe signals from the capture region and from locations just above and below the capture region that were recorded during a shot. Here  $t = 0 \mu\text{s}$  again corresponds to the start of the PI bank discharge, while the Main bank discharge begins at  $t \sim 16.9 \mu\text{s}$ . There are consecutive peaks in the T2, T3, T5, and T6 waveforms marking the FRC's passage. A slight transition in slope is seen in the T4 waveform where a corresponding peak should be, as the FRC begins retracting from the T6 location at this time, while the end of the FRC continues its translation into the capture region. The peak in the T4 signal then occurs when the reversing front of the FRC meets the still-advancing tail. The T4 signal ends up being the largest and broadest among the other B-dot signals because the magnetic field between the mirrors is lowest and the FRC is able to expand the most here.

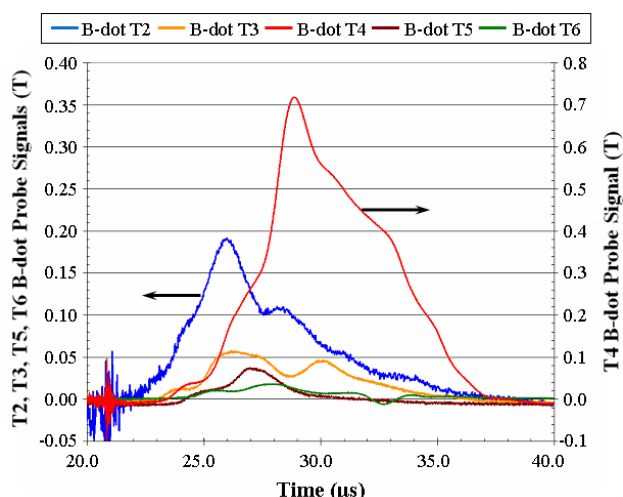


Figure 8. B-dot probe measurements just below (“T2”), within (“T3”, “T4”, and “T5”), and just above (“T6”) the capture region. The noise seen at  $\sim 21 \mu\text{s}$  is due to the Main bank Crowbar switch trigger.

That the FRC is captured is evident from the long duration of the T4 signal. The shoulder at  $\sim 33 \mu\text{s}$  is a typical feature and indicative of the onset of a process that accelerates the decay of the FRC (e.g., perhaps through instability). The appearance of the T6 signal, which again is outside the capture region, indicates that the FRC stretches beyond the upper mirror, and though the front returns to the capture region, there is the likelihood of mass (and flux) loss occurring as it stretches into this region of diverging fields. In addition, the T2 signal has a much slower decline than should be appropriate if the FRC simply passed by, and it persists throughout the duration of T4 signal. This is not a typical feature, and suggests that in this shot the FRC did not fully enter the magnetic well but split into two parts. Another possibility is that it stretched past the lower mirror after its reflection much as it stretched past the upper mirror earlier. In any case, these phenomena are suggestive of improvements to the mirror profile being needed.

#### IV. EFFORTS TO INCREASE LIFETIME

Several simultaneous approaches are being actively investigated to lengthen FRC trapped-flux lifetime. In addition to simply varying (or “tuning”) bank parameters (e.g., bank voltages, trigger timings, gas puff delays, etc.) an RF “pre-pre-ionization” system was developed to promote breakdown of the  $\text{D}_2$  when a greater amount of the Bias field is present in the theta coil. Axial plasma injection with a plasma gun has been investigated at an exploratory level as a means of improving stability during translation and capture, but this work will be discussed in a future paper. A more in-depth effort to develop an active rotation control method to promote FRC stability against the “ $n=2$ ” rotational build-up has been ongoing and will be discussed here. Lastly, changes in the Mirror field profile have been explored recently, and these efforts have led to the largest improvements in FRC lifetime.

##### A. Improved Breakdown, Flux Capture via Pulsed RF Fields

The difficulty with ringing theta pinch pre-ionization is that it induces breakdown in the  $\text{D}_2$  gas via an azimuthal electric field, which must act transverse to the Bias field. If an axial electric field could be applied, the insulating effect of the Bias field would not be an issue. Based upon this observation and reported improvements in past experiments [11] when using axial electric fields, a charged-cable pulser was constructed to generate large-amplitude, short-duration, axial electric fields (a few 10's of kV at  $\sim 30 \text{ MHz}$  for 10's of ns) to break down the  $\text{D}_2$  gas or, alternatively, to assist the PI bank in breaking down the gas when a larger percentage of the Bias field is present [12]. The RF fields are applied between two copper split-ring electrodes placed at the top and bottom of the formation region, inside the theta coil but outside the quartz tube [7, 12]. Figure 9 shows photos of one of the electrodes and its placement within the theta coil structure.



Figure 9. (left) close-up view of one of the split-ring RF electrodes; (right) the electrode is seen near the bottom of the partially assembled theta coil, with two flux loop rings above it.

Figure 10 shows the FRC excluded flux radii at the top of the theta coil (“Rexc,J”) and in the center of the capture region (“Rexc,T4”) for a pair of tests that compare the use of the RF fields. For the test with the fields, the charged-cable pulser was triggered  $\sim 13.2 \mu\text{s}$  after the PI bank discharge and  $\sim 3.7 \mu\text{s}$  before the Main bank discharge. In this case the PI bank had already broken down the gas, and the cable pulser was discharged in an attempt to entrain additional flux prior to the Main bank discharge.

The slight increase in radius for the test with RF fields

implies that more flux was indeed entrained within the FRC during formation, and while the increase is very modest, it demonstrates the validity of the concept. That larger increases in excluded flux radius (or in trapped flux lifetime) have not been observed appears to be due to the RF fields lacking sufficient energy to produce a greater degree of ionization. With more energetic axial fields it should be possible to substantially increase the amount of background Bias field trapped within this plasma.

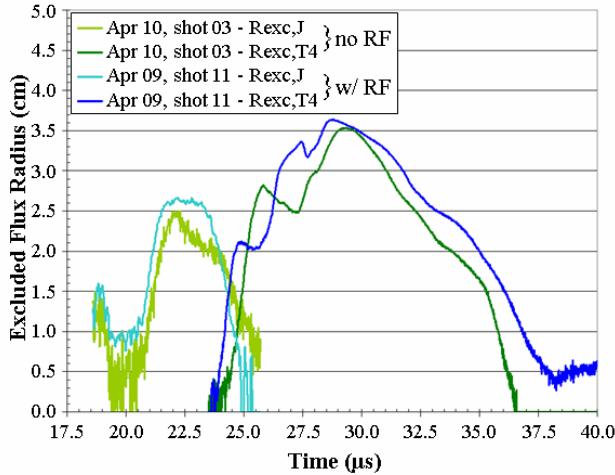


Figure 10. Comparison of the calculated excluded flux radii from tests with and without axial RF electric fields.

### B. Measures to Improve FRC Stability

To improve FRC stability, a system has been developed consisting simply of a biased ring placed above the solid liner and the upper mirror coils in a region where the field lines rapidly diverge and intersect the walls of the system. The theory of operation is as follows. An FRC, once formed, starts to rotate due, in part, to the plasma conditions (lower temperature, higher density) at the vacuum chamber wall where the open magnetic field lines exit the system. The Generalized Ohm's Law  $\nabla p_e$  term in the electric field implies that a non-rotating FRC will have an electric field crossing the magnetic field lines at the wall [13]. Whether the wall is a dielectric material or a metal, the conductivity of the wall or plasma layer that develops there will carry current and eventually short out this electric field. This current and its associated magnetic field then introduce torque at the separatrix and cause an unstable viscous sheared flow across the separatrix, which leads to rotation of the FRC [14]. Supporting this electric field with an external circuit coupled to a conducting ring placed in the magnetic field exit region, as illustrated on the left in Figure 11, should prevent rotation [15].

The illustration on the right of Figure 11 shows the implementation of the biased ring on FRCHX, which in some ways is like a plasma gun, and Figure 12 shows its driving circuit. A single Main Ring (A) is placed ~15 cm above the solid liner, and seven cables connect it to a charged capacitor bank. A Trigger Ring (B), located between the Main Ring and the top Ground Plate (C), enables the ring circuit to be

discharged upon command if there is sufficient gas in the ring region. Alternatively, a plasma gun can trigger the ring circuit by injecting conducting plasma between the Main Ring and the Ground Plate. As the energy in the ring circuit discharges through the gas or plasma in the region, additional neutral gas is ionized, and the current-carrying plasma is heated and expands back along the open magnetic field lines into the capture region, carrying with it not only the discharge current but the electric field needed for stabilization (as shown in Figure 11), as well. Early experimental results with the biased ring assembly showed inconclusive results with regard to enhancements in trapped flux lifetime. Limited testing after the magnetic well was widened (to be discussed next) has shown a slightly more substantial effect on the trapped flux lifetime, with increases of 5~10 % being observed. This suggests that the rotation control measures are having an effect.

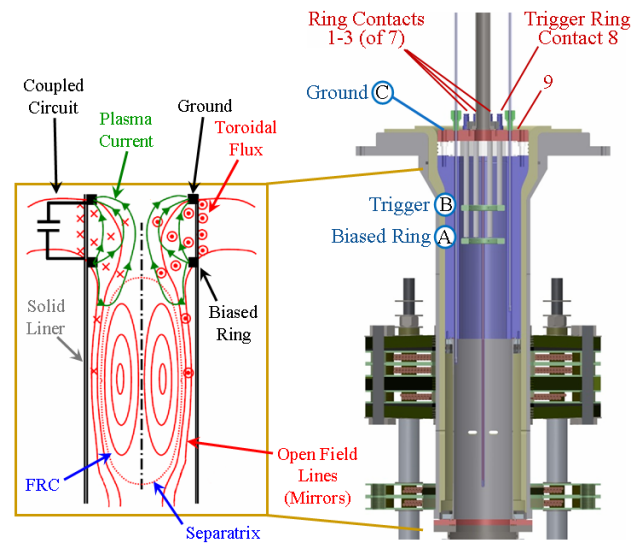


Figure 11. (left) Illustration showing the interaction between the biased ring circuit and the FRC; (right) implementation of the biased ring concept on FRCHX.

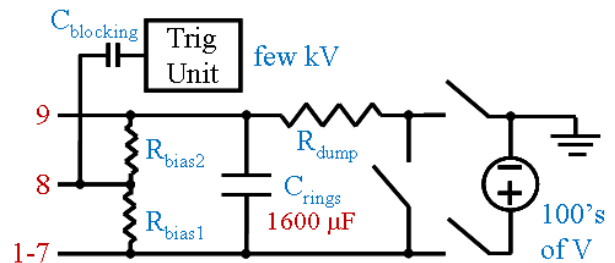


Figure 12. The driving circuit for the biased ring.

### C. Modifications to Capture Region Fields

Efforts to improve the capture region magnetic field profile have centered on increasing the volume in the magnetic well by either deepening the well (to allow a fatter, more stable FRC to be held) or lengthening it (to better match the prolateness of the FRC, which also improves its stability). Several iterations of numerical studies have been performed to

examine how the magnetic well could be deepened while generally keeping the mirror field peaks in the same locations and at the same amplitudes. The most promising path for achieving this goal involves placing a metallic flux excluding plate between the lowest upper mirror coil and the other two upper mirror coils [16]. A 25% decrease in the field minimum can be obtained according to the calculations for this case. Some decrease in the mirror field peaks (5% for the lower mirror and 10% for the upper mirror) also results, but the mirror amplitudes can be restored by adding more windings to the coils or, in the case of the upper mirror, by adding another complete coil above the existing coils.

Though not entirely suited for the existing solid liner, the mirror coils were spread apart by  $\pm 5$  cm relative to one another, as illustrated in Figure 13, in order to test the effects of a longer capture region. Because of magnetic diffusion and other factors, the peak fields move apart by only 3 cm in each direction, but the change is sufficient to produce noticeable effects on FRC capture.

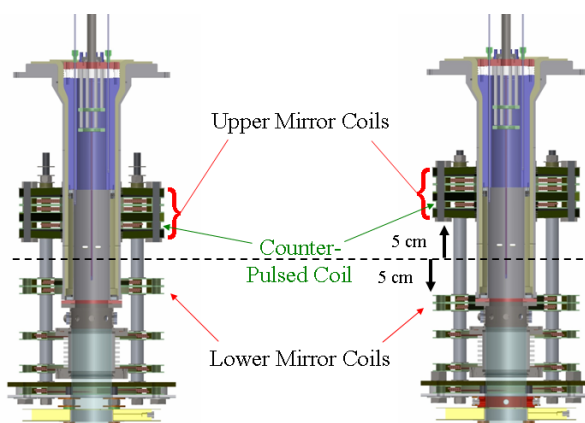


Figure 13. Illustration of the translation and capture regions of FRCHX before (left) and after (right) the mirror coils were repositioned.

Indeed, results from tests with the wider magnetic well have shown the greatest improvements in trapped flux lifetimes so far, with measurements of full-width, half-maxima of the excluded flux radii in the capture region jumping from  $8 \sim 11 \mu\text{s}$  to  $14 \sim 16 \mu\text{s}$ . Figure 14 provides a comparison between two shots performed prior to widening the mirror spacing and two shots performed afterwards. In all cases the PI bank discharge was at  $t = 0 \mu\text{s}$ , and the Main bank discharge was at  $t = 16.9 \mu\text{s}$ . As can be seen, shots 12 and 13 from May 16 show a width that has jumped to  $\sim 14 \mu\text{s}$ . Also, the sudden drop in excluded flux radius (at  $t = 31 \sim 32 \mu\text{s}$ ) following the peak is now curtailed, giving way to a more exponential decay (which is largely responsible for the increased lifetime). As noted in the previous sub-section, limited testing with this wider capture region and with a voltage placed on the biased ring has shown still further incremental improvements to the lifetime. These results strongly suggest that there is room for even more improvement with an even longer magnetic well.

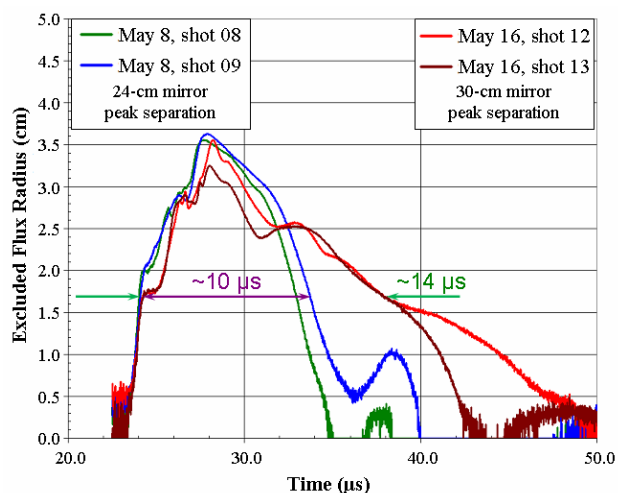


Figure 14. Comparison of excluded flux radii at the middle of the capture region before and after the widening of the magnetic well.

## V. MODELING AND SIMULATION

Greater agreement between MACH2 calculations and experimental data has been achieved in recent months by using the time at which the first visible light emissions are observed by the optical fiber probes in the FRCHX formation region (i.e., the “time of first light”) as an indicator of when ionization and flux-trapping should begin in the simulations. This technique produces capture region integrated B-dot signatures that are much like those measured in the corresponding experiments. It therefore highlights the importance of the breakdown processes, their timing, and the amount of flux trapped in the FRC during formation.

With this improved agreement, MACH2 results have been able to provide better understanding of the underlying physics associated with the diagnostic measurements obtained, specifically how well (or not) the FRC is captured between the magnetic mirrors given the recorded magnetic probe data, and how much mass and flux is likely lost during a poor capture. By including the liner compression in such simulations, it is possible to go one step further and obtain estimates of the degree to which FRC capture may be affected by the imploding solid liner, specifically how much less or greater the mass and flux loss may be depending upon when the FRC is injected during the implosion.

To maximize the FRC lifetime within the imploding liner, it is useful to have the liner walls already accelerating inward when the FRC arrives. As was noted back in Section II, there is very little change to the liner radius during the first  $4 \mu\text{s}$  of the implosion, and by  $10 \mu\text{s}$  the radius has decreased only  $\sim 3.5$  mm or  $\sim 7\%$ . Figure 15 shows a set of plots from MACH2 calculations based upon the “first light” and other experimental parameters from one of the FRCHX tests. For this simulation, a  $5.65 \mu\text{s}$  delay was introduced between the start of the liner implosion and the Main bank discharge. The FRC then arrived at the liner  $\sim 12 \mu\text{s}$  into the implosion. The liner’s radius is  $\sim 80\%$  of its original  $4.89$  cm at this time, and the mirror fields have increased by  $64\%$ . Only a fraction of

this FRC was captured, as is evident from the 14- $\mu$ s plot.

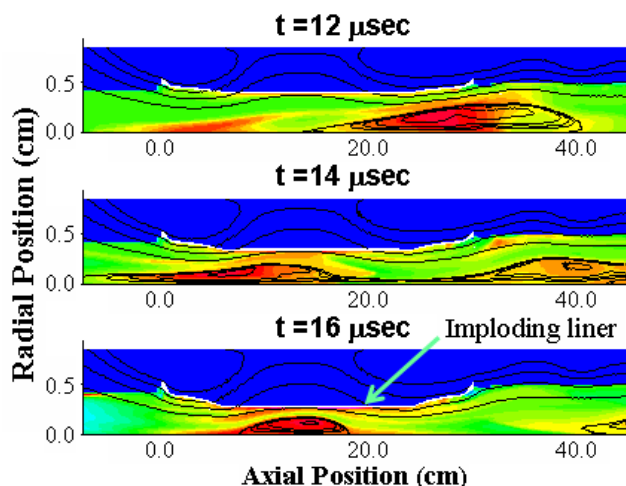


Figure 15. MACH2 density contour plots showing FRC injection (from right) and capture during liner implosion. The black lines show surfaces of constant magnetic flux density; the times are relative to Main bank discharge.

The MACH2 simulations have underscored the fact that the amount of flux trapped during pre-ionization, and hence entrained in the FRC during formation, affects the FRC lifetime and robustness. A compression simulation similar to Figure 15 but starting with “first light” data from another experimental test in which the pulsed axial electric fields described in Section IV.A. were used to increase flux trapping produced an FRC with 67% more flux after its formation (1.257 mWb vs. 0.754 mWb). As a result, more of the FRC was captured in the imploding liner, and at that time it had more flux (0.415 mWb vs. 0.346 mWb), was hotter (273 eV vs. 209 eV), was less dense ( $n_i = 2.6 \times 10^{16} \text{ cm}^{-3}$  vs.  $3.3 \times 10^{16} \text{ cm}^{-3}$ ), was captured sooner (but a slightly earlier capture means less compression has occurred), and had a factor of 25 higher neutron yield at a 5 mm liner radius ( $2 \times 10^9$  vs.  $8 \times 10^7$ ). Thus, increasing trapped flux in the FRC during formation is important for more reasons than just lengthening FRC trapped-flux lifetime.

## VI. DISCUSSION AND SUMMARY

Given the correlation brought to light by the modeling between the amount of magnetic flux trapped in the FRC and its temperature and density at capture, and the resulting neutron yield at the final stages of compression, it is apparent why lengthening the lifetime of the trapped flux in the FRC is important. The calculated waveforms in Figure 3 further highlight the significance of the final microseconds of the compression, as due to the volumetric nature of the FRC temperature and density the greatest increases in these quantities, like the magnetic flux density, will be obtained as the liner approaches its minimum radius. Thus, the lifetime of the trapped flux in the FRC should ideally be such that the trapped flux does not simply persist until the compression is almost complete, but rather there should be a significant amount of trapped flux that persists within the FRC through

the entire duration of the compression. The various paths being explored to lengthen the FRC trapped flux lifetime – application of axial RF electric fields for better control of plasma breakdown and flux trapping, efforts to actively support the electric fields at the ends of the open magnetic field lines to maintain FRC stability, and modifying the magnetic field profile in the capture region (specifically, widening the magnetic well) – have been successful in gradually raising the lifetime, with the latter yielding the greatest improvements thus far. Trapped flux lifetimes of FRCHX FRCs, as measured from the half maximum of the increasing exclusion radius in the formation region to the half maximum of the decreasing exclusion radius in trapped region now easily range from  $\sim 19 \mu\text{s}$  to  $\sim 21 \mu\text{s}$ . The analogous measure of lifetime just in the trapping region is  $14 \sim 16 \mu\text{s}$ . Lifetimes have been observed to be longer still with moderate bias voltages placed on the biased ring assembly.

With an axially longer magnetic well, the decrease of the exclusion radius and corresponding fast magnetic field component is more exponential in appearance rather than an abrupt drop, as was almost always the case prior to widening the well. This change suggests that the end-of-lifetime mechanism for the FRC is more likely due to resistive decay of the trapped flux now, rather than some other mechanism. The resistive decay may possibly be enhanced by cooling of the plasma from the introduction of impurities over time in capture region from the quartz sleeves around the biased ring or the B-dot probes, and thus if impurities can be minimized even longer lifetimes may be possible.

Recent 2D-MHD simulations are giving confidence in the likelihood of success with increased delays between the start of the liner compression and the start of FRC formation. This is facilitated by the initially slow inward acceleration of the liner radius right after the start of the implosion drive discharge and separate banks driving the Translation and Mirror coils. The latter allows lower mirror field amplitudes to be established during a compression tests compared to a static-capture test, as the imploding liner will begin to increase the mirror fields while the FRC is forming and translating. Such timing changes may remove as much as  $8 \mu\text{s}$  from the lifetime requirement for the FRC, reducing the original  $\sim 25\text{-}\mu\text{s}$  requirement to  $\sim 17 \mu\text{s}$ . The present simulations show that even though there is not complete capture of the FRC under such conditions, using the increased delays together with the increased lifetime will allow us to attempt the next compression shot.

## REFERENCES

- [1] K. F. Schoenberg, R. E. Siemon, et al, “Magnetized Target Fusion, A Proof of Principle Research Proposal”, LA-UR-98-2413, 1998, [http://wsx.lanl.gov/Proposals/mtf\\_pop\\_proposal.pdf](http://wsx.lanl.gov/Proposals/mtf_pop_proposal.pdf).
- [2] J. M. Tacetti, T. P. Intrator, et al, Rev. Sci. Instr., vol. 74, pp. 4314-4323, 2003.
- [3] G. A. Wurden, T. P. Intrator, et al, "FRCHX Magnetized Target Fusion HEDLP Experiments", in Proc. IAEA 2008 Fusion Energy Conference, IAEA-CN-165, IC/P4-13, Geneva, Oct 13-18, 2008.
- [4] J. H. Degnan, D. J. Amdahl, et al., “Experimental and Computational Progress on Liner Implosions for Compression of FRCs,” IEEE. Trans. Plasma Sci., vol. 36, p. 80-91, 2008.
- [5] J. H. Degnan, P. Adamson, et al, “Field reversed configuration (FRC) formation and compression,” in Proc. 2008 International Conference on

Megagauss Magnetic Field Generation and Related Topics, 2010, p. 522-531.

- [6] C. Grabowski, J. H. Degnan, et al., "FRC Lifetime Studies for the Field Reversed Configuration Heating Experiment (FRCHX)," in Proc. 18th IEEE Pulsed Power Conference, 2011, p. 431.
- [7] C. Grabowski, J. H. Degnan, et al., "Extending Field-Reversed Configuration Lifetime for High Energy Density Plasma Experiments," presented at 39th IEEE International Conference on Plasma Science, Edinburgh, UK, July 8 – 12, 2012.
- [8] J. H. Degnan, D. J. Amdahl, et al., "Recent Magneto Inertial Fusion Experiments on the Field Reversed Configuration Heating Experiment", submitted to Nuclear Fusion, Dec. 2012.
- [9] T. S. Greene, "Evidence for the Containment of a Hot, Dense Plasma in a Theta Pinch," Rev. Sci. Lett., vol. 5, pp. 297-300, 1960.
- [10] M. Tuszewski, "Field Reversed Configurations," Nucl. Fus., vol 28, pp. 2033-2092, 1988.
- [11] A. L. Hoffman and J. T. Slough, "Field Reversed Configuration Lifetime Scaling Based on Measurements from the Large S Experiment," Nucl. Fus., vol. 33, pp. 27-38, 1993.
- [12] G. F. Kiuttu, M. R. Kostora, et al., "RF Pre-Preionization for the FRCHX Experiment," presented at the 39th IEEE International Conference on Plasma Science, Edinburgh, UK, July 8 – 12, 2012.
- [13] L. C. Steinhauer, "End-Shorting and electric field in edge plasmas with application to field-reversed configurations," Phys. Plasmas, vol. 9, pp. 3851, 2002.
- [14] E. L. Ruden, "The FRC's  $n=2$  rotational instability interpreted as the dominant Rayleigh-Taylor mode of a gyroviscous plasma with sheared toroidal flow," presented at the US-Japan CT Workshop 2004: New Directions and Physics for Compact Toroids, Santa Fe, NM, Sept. 14-16, 2004.
- [15] E. Ruden and M. Frese, "FRC rotation control using an electric field," presented at the 49th Annual meeting of the Division of Plasma Physics, Orlando, FL, Nov. 12-16, 2007.
- [16] M. T. Domonkos, D. Amdahl, et al., "Applied Magnetic Field Design for the FRC Compression Heating Experiment (FRCHX) at AFRL," Rev. Sci. Instrum., vol. 84, 043507, 2013.